Pyrite depression by dextrin in flotation with xanthates. Adsorption and floatability studies

Alejandro López-Valdivieso [1], Aldo A. Sánchez-López [1], Erika Padilla-Ortega [2], Aurora Robledo-Cabrera [1], Edelmira Galvez [3], Luis Cisternas [4]

[1] Instituto de Metalurgia, Laboratorio de Química de Superficies, Universidad Autónoma de San Luis Potosí, Av. Sierra Leona 550, San Luis Potosí, SLP, 78210 México.

[2] Centro de Investigación y Estudios de Posgrado, Facultad de Ciencias Químicas, Universidad Autónoma de San Luis Potosí, San Luis Potosí, S.L.P., 78260 Mexico

[3] Departamento de Ingeniería Metalúrgica y Minas, Universidad Católica del Norte, Avenida Angamos 610, Antofagasta, 1240000 Chile.

[4] Departamento de Ingeniería Química y Procesos de Minerales, Universidad de Antofagasta, Avenida Angamos 601, Antofagasta, 1240000 Chile

Corresponding author: alopez@uaslp.mx (Alejandro López-Valdivieso)

Abstract: Depression of pyrite by dextrin in flotation with xanthates has been studied. The adsorption of dextrin and xanthates at the pyrite/aqueous solution interface has been investigated through electrokinetics, Raman spectroscopy and batch adsorption studies using oxidized pyrite. Microflotation studies were undertaken to evaluate the pyrite depression with dextrin using ethyl and propyl xanthates as the collector. The surface density of ferric hydroxide on pyrite depended on pH and was highest about the iep (pH 7.5) of the oxidized pyrite. Dextrin adsorption was directly related to the surface density of ferric hydroxide and took place through two steps suggesting two adsorption mechanisms on ferric hydroxide. Xanthate adsorption as dixanthogen occurred along with ferric hydroxide dissolution causing partial dextrin desorption from the pyrite surface; consequently, co-adsorption of xanthate and dextrin occurred on the surface. Depression of pyrite flotation with xanthate was determined by the oxidation level of the pyrite surface. Floatability of pyrite with xanthate was highly impaired by dextrin at pH 8 only when the surface density of ferric hydroxide on the pyrite surface was very high.

Keywords: pyrite, dextrin, adsorption, flotation, xanthates, polysaccharides

1. Introduction

Dextrin is environmentally safe regulator with the potential to replace toxic cyanide for the depression of pyrite in base-metal sulfide flotation (Laskowski et al., 1993; Rath et al., 1999; Lopez Valdivieso et al., 2004). Pyrite depression with dextrin occurs around pH 8 so using dextrin could lower the pH in flotation processes operating at high pH such as the flotation of copper in porphyry ores and flotation of zinc in polymetallic base-metal sulfide ores. Furthermore, dextrin could be used as a pyrite depressant in copper flotation plants using sea water where high pH is unpractical because of the high amount of lime that it would be required (Castro, 2012). Dextrins are commercially used for depression of carbonaceous pyrite in copper flotation, depression of lead in lead-copper bulk separation (Bulatovic, 2007) and depression of hematite and apatite in their reverse flotation against siliceous minerals (Lin and Burdick, 1988). Dextrin dosages of up to 1,400 g/Mg is reported.

Adsorption of dextrin is very low on non-oxidized pyrite (Bogusz et al., 1997) and high on pyrite with iron hydroxide on the surface (López Valdivieso et al., 2003, 2004). This iron hydroxide that is formed from the oxidation of the pyrite enhances dextrin adsorption, which is maximum at pH values

close to the pHiep 7.5 of the oxidized pyrite. The surface oxidation of pyrite has been extensively studied by various techniques such as cyclic voltametry, Raman spectroscopy, X-ray photoelectron spectroscopy (Buckley and Woods, 1984; Todd et al., 2003). They all have reported the formation of ferric oxyhydroxide species on the surface. Electrokinetics has also been used to study the surface oxidation of pyrite (Fuerstenau et al., 1968, 1990; Fornasiero and Ralston, 1992; Kydros et al., 1994; Bulut et al., 2004). Pyrite prepared under an oxygen-free atmosphere shows an isoelectric point below pH 2. Upon oxidation, pyrite presents two additional isoelectric points between pH 4 and 8.6 due to ferric hydroxide on the pyrite surface. Through atomic force microscopy studies Miller et al., (2002) and Hochella (2003) found that the ferric hydroxide formed as patches on the pyrite surface.

Xanthates are common collectors in flotation of base-metal sulfide ores. In these ores, pyrite is the major sulfide gangue so its flotation has to be impaired to produce high quality base-metal sulfide concentrates. In lead flotation, pyrite depression is undertaken with inorganic reagents, namely cyanide, ferricyanide and sulfite salts (Ball and Rickard, 1976; Kydros et al., 1994; Bulatovic and Wyslousil, 1995). While in zinc and porphyry copper flotation high pH, adjusted with lime, is the route to depress pyrite. The inorganic reagents and lime prevent xanthate adsorption on the pyrite surface (Ball and Rickard, 1976; Chander, 1988; Bulatovic and Wyslousil, 1995). Dextrin does not prevent xanthate adsorption on pyrite, but it turns the pyrite surface hydrophilic by enclosing adsorbed collectors (López-Valdivieso et al., 2003, 2004).

The aim of this work was to delineate the adsorption mechanisms of dextrin onto pyrite surface and the role of sulfhydric collectors on the adsorption and to establish proper conditions for the use of dextrin as an effective pyrite depressant in flotation of sulfides. Ethyl and propyl xanthates have been used as the representative of the sulfhydric collectors. The effect of the oxidation state of the pyrite surface on the dextrin adsorption and pyrite floatability was assessed. The chemical species formed on the pyrite surface as a result of oxidation and adsorption of dextrin and xanthate were characterized by electrokinetics and Raman spectroscopy.

2. Experimental

2.1. Materials and reagents

Natural specimens of pyrite from Zacatecas, Mexico were used in this investigation. Large pieces of pyrite were first crushed to –635 μm, then purified through the removal of quartz, calcite and other sulfide impurities by hand sorting under an optical microscope. From this sample, two distinct size fractions were prepared, –75+45 μm for microflotation tests and –38 μm for adsorption and electrokinetic tests. The specific surface area of the –38 μm particles was determined by the BET method using a Micromeritics ASAP 200 Specific Surface Area Meter and was found to be 0.81 m^2/g. Potassium ethyl (PEX) and sodium propyl (SPX) xanthates were obtained from Alkemin, Mexico, with a purity higher than 90%. These xanthates were further purified threefold by dissolution in acetone followed by crystallization in ethylic ether. The dextrin was the Tapioca Dextrin 12, from A. E. Staley Manufacturing Co. The molecular weight of this dextrin has been reported to be 56,000 (Nyamekye and Laskowski, 1993). All aqueous solutions were prepared using deionized water and the inorganic reagents were all analytical grade.

Adsorption, electrokinetics, Raman spectroscopy and floatability studies were carried out with pyrite, whose surface was oxidized at two distinct levels. This was achieved by agitating pyrite-water suspensions at two distinct periods of time, namely 30 min and 24 hs, in a beaker open to the atmosphere. The short and long period of time were selected in order to have a big difference in the oxidation level of the pyrite surface.

2.2. Ferric hydroxide analysis on pyrite surface

Ferric hydroxide on the pyrite surface was determined by dissolution with EDTA, a technique that selectively leaches iron oxides of the pyrite surface (Wang and Forssberg, 1990; Clarke et al., 1995; Rumball and Richmond, 1996). Pyrite/water suspensions were prepared with one gram of –38 μm pyrite in 100 ml aqueous solution. The suspensions were stirred in a beaker open to the atmosphere for 30 min and 24 hs. Afterwards, the suspension pH was adjusted to the desired value and stirred for a

further 30 min. Following this step, the suspension was brought into a globe box with a nitrogen atmosphere for extraction of ferric hydroxide from the pyrite surface by EDTA. An EDTA aqueous solution was added to the suspension for a 0.05 mol/dm^3 EDTA concentration and the suspension was stirred for another 30 min. Then, a 20 mL supernatant was withdrawn and placed into a centrifuge tube with a lid for centrifugation, which was performed out of the glove box. The supernatant was assayed for total iron by atomic absorption spectrophotometry using a Perkin Elmer apparatus. The iron concentration was converted to ferric hydroxide, $Fe(OH)_3$, and reported as such in this work.

2.3. Microflotation and adsorption studies

Microflotation tests were carried out using a modified Hallimond tube (Fuerstenau et al., 1957). For these tests pyrite/water suspensions were prepared with one gram pyrite and 100 ml aqueous solution. Prior to flotation, the pyrite was oxidized for 30 min and 24 hs. After this step, the suspension pH was adjusted to the desired value with dilute solutions of HCl and KOH and the mineral was conditioned at this pH for 30 min. Then, xanthate was added to the suspension at the desired concentration and contacted with the pyrite for 30 min. Afterwards the suspension was transferred to the Hallimond tube for actual flotation for one min using nitrogen at a flow rate of 30 mL/min. When dextrin was used, it was added before the collector and contacted with the mineral for 5 min.

Adsorption of dextrin and xanthate was carried out with one gram of –38 μm particles in 100 ml aqueous solution. The mineral was first oxidized as mentioned above, then conditioned at the desired pH with the collector and dextrin concentration following the sequence of reagent addition as in the flotation tests. After contacting the mineral with dextrin and collector, the suspension was centrifuged at 3900 rpm for 15 min and a 20 mL aliquot was withdrawn from the supernatant for chemical analysis of dextrin and xanthate. Xanthate was determined by UV-VIS Spectrophotometry using a UV Beckman DU 650 at 301 nm wavelength (Leja, 1982). Dextrin was analyzed using the Dubois technique (Dubois et al., 1956).

2.4. Raman spectroscopy surface characterization and zeta potential determination

Raman spectroscopy analysis was carried out with of –38 μm particles of non-oxidized pyrite, oxidized pyrites and oxidized pyrites treated with dextrin and xanthate at using a Micro-Raman laser spectrometer (Thermo Scientific, laser DXR 532 nm), with a scanning range between 50 and 3500 cm^{-1} and at a laser power of 10 mW.

Electrokinetic measurements were performed using a Coulter Delsa 440 Zetameter with suspensions prepared at 0.1%w solid. The mineral was first oxidized as mentioned above, then the suspension pH was adjusted to the desired pH, followed by the addition of collector and dextrin, using the same sequence of reagent addition as in the flotation tests. After conditioning, about 5 ml of the suspension was transferred to the electrophoretic cell for electrokinetic mobility measurements, which were transformed to zeta potential using the Smoluchouski Equation.

3. Results and discussion

3.1. Ferric hydroxide on pyrite

Figure 1 shows the surface density of ferric hydroxide on pyrite as a function of pH after oxidation for 30 min and 24 hs. As seen, the surface density of ferric hydroxide increased with the oxidation time. About 80 μmol/m^2 ferric hydroxide formed within the pH range of 6 to 10 for the oxidation time of 24 hs and 55 μmol/m^2 within the pH range of 8 to 10 for the shortest oxidation time of 30 min. This pH range of highest ferric hydroxide formation on pyrite is in good agreement with Wang and Forssberg (1990).

Raman spectroscopic characterization confirmed that more ferric hydroxide formed on the pyrite surface for the longest oxidation time of 24 hs. Figure 2 shows the Raman spectra of pyrite: (a) with no oxidation treatment, (b) oxidized for 30 min and (c) oxidized for 24 hs. It is noted that the pyrite spectrum showed three main bands at 340, 380 and 429 cm^{-1} corresponding to the Fe-S covalently-bonded of pyrite (Parker and Hope, 2010). The spectra of the oxidized pyrites revealed significant differences in the range of 400 and 900 cm^{-1} where intense bands corresponding to Fe-OH (796, 740, 720

and 481 cm^{-1}) vibrations appeared (Sitter et al., 1988; Stone et al., 2006; Das and Hendry, 2011) confirming the presence of ferric hydroxide on the pyrite surface. The intensity of these bands augmented with the oxidation time. Moreover, the bands with low intensity at 557 and 549 cm-1 demonstrated the existence of ferric oxide on the pyrite surface
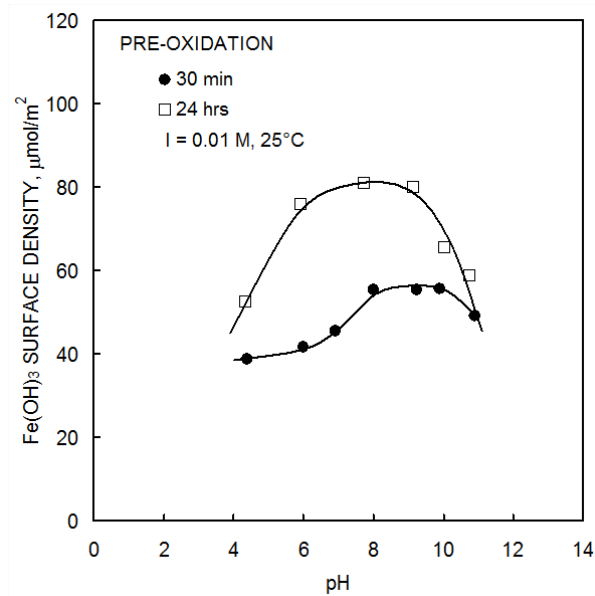

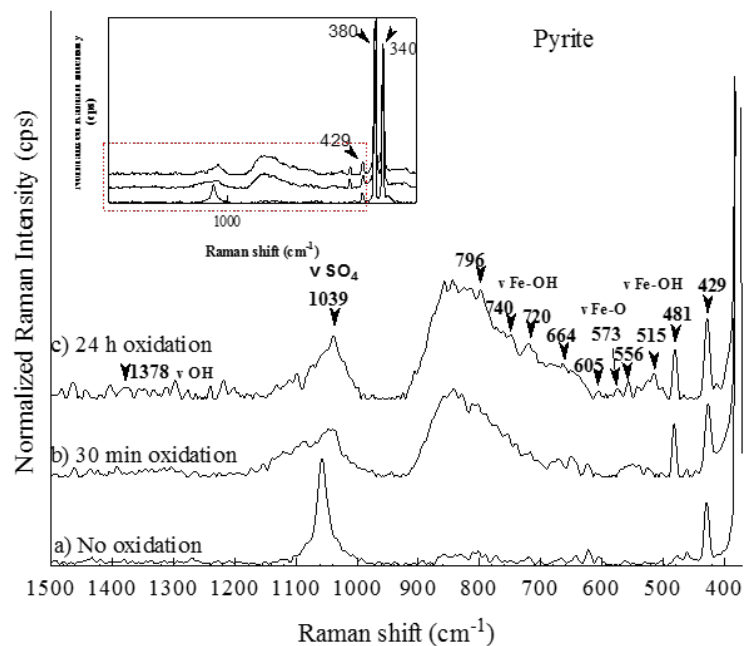Fig. 1. Surface density of ferric hydroxide (Fe(OH)$_3$) as a function of pH on pyrite oxidized for 30 min and 24 h

Fig. 2. Raman Spectrum of pyrite: (a) no oxidation treatment, (b) oxidized for 30 min and (c) oxidized for 24 h

3.2. Dextrin adsorption on oxidized pyrite

Dextrin adsorption as a function of pH on the oxidized pyrites is presented in Figure 3, using an initial dextrin concentration of 400 mg/dm^3. It can be noted that dextrin adsorption was higher on the pyrite with the greater surface density of ferric hydroxide. Dextrin adsorption was maximum about the iep of the oxidized pyrite, pH 7.5. There is a direct relationship between dextrin adsorption and the surface density of ferric hydroxide on pyrite as seen in Fig. 4.
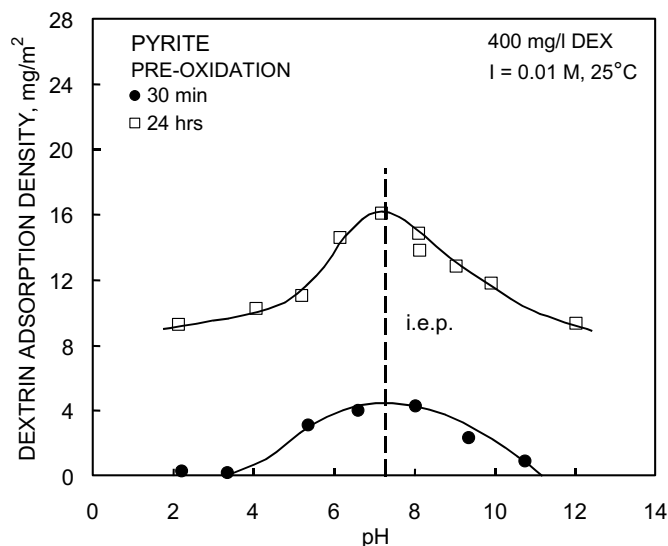
Fig. 3. Dextrin adsorption on pyrite oxidized for 30 min and 24 h as a function of pH in the presence of 400 mg/dm³ dextrin
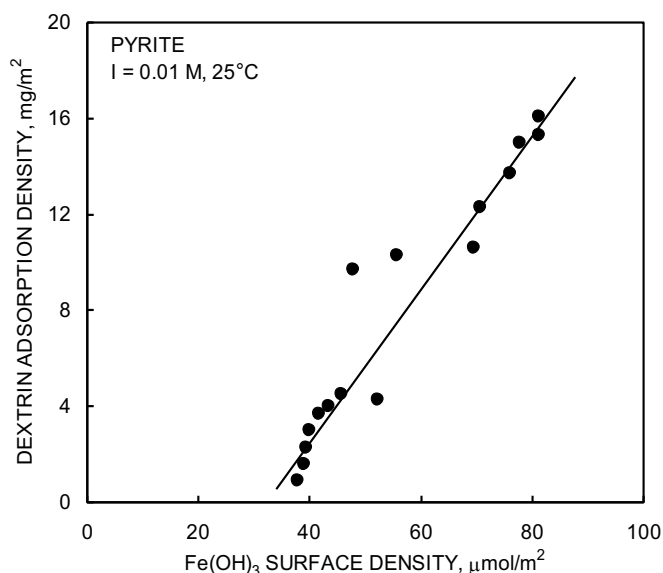

Fig. 4. Dextrin adsorption of pyrite as a function of surface density of ferric hydroxide (Fe(OH)₃)

Figure 5 depicts the zeta potential of pyrite as a function of pH in the absence and presence of two distinct dextrin concentrations, namely 50 and 100 mg/dm³. Pyrite shows two isoelectric points, namely at pH 3.5 and 7.5. This is due to ferric hydroxide on the pyrite surface, as reported elsewhere (Fuerstenau et al., 1968; Lopez-Valdivieso et al., 2005). Dextrin turned the positive zeta potential of pyrite to negative, indicating that dextrin specifically adsorbed on pyrite. Ferric hydroxide on the pyrite enhanced the adsorption, which involves the interaction of surface Fe(III)(OH) sites with the OH groups of the C2 and C3 carbon in the glucose units of the polysaccharide (Wiessenborn, 1993; Lui and Laskowski, 1989, 2002). Dextrin may also affect the electrokinetic shear plane at the pyrite/aqueous solution interface causing a decrease in the magnitude of the zeta potential.

The Raman spectra of the oxidized pyrite in the absence (a) and presence of dextrin (b) are presented in Figure 6. The Raman spectrum of the oxidized pyrite in the presence of dextrin showed strong bands at 1094, 1350, 1650 cm⁻¹ due to v–CCO, v–OH, v–C=C bonds, respectively, corresponding to dextrin (Das et al., 2016). This revealed the presence of dextrin on the surface of the oxidized pyrite. Comparing the spectra, it can be noted that in the pyrite with dextrin the bands corresponding to v–Fe-O at 557 and

549 cm^{-1} increased in intensity while the bands at 720 and 796 cm^{-1} attributed to ν–Fe-OH almost disappeared. This supports that dextrin binds with Fe-OH groups of the ferric hydroxide with the release of protons.

Dextrin adsorption isotherms of the oxidized pyrites at pH 8, where high adsorption of dextrin took place, are depicted in Fig. 7. Adsorption of dextrin was greater on the pyrite oxidized for 24 hs than that
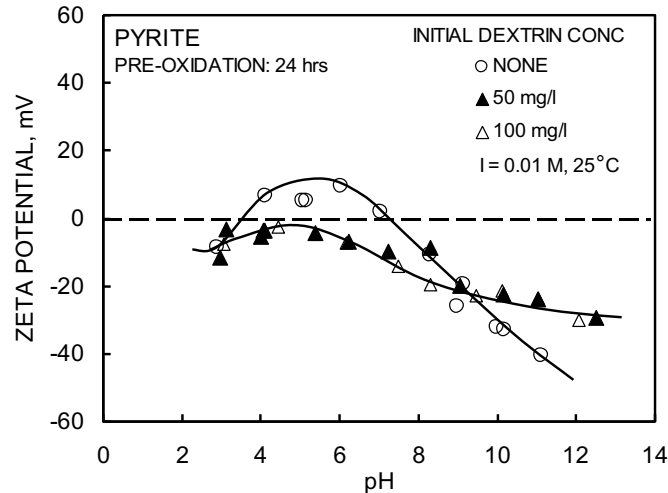

Fig. 5. Zeta potential of pyrite oxidized for 24 h as a function of pH in the absence and presence of 50 and 100 mg/dm^3 dextrin
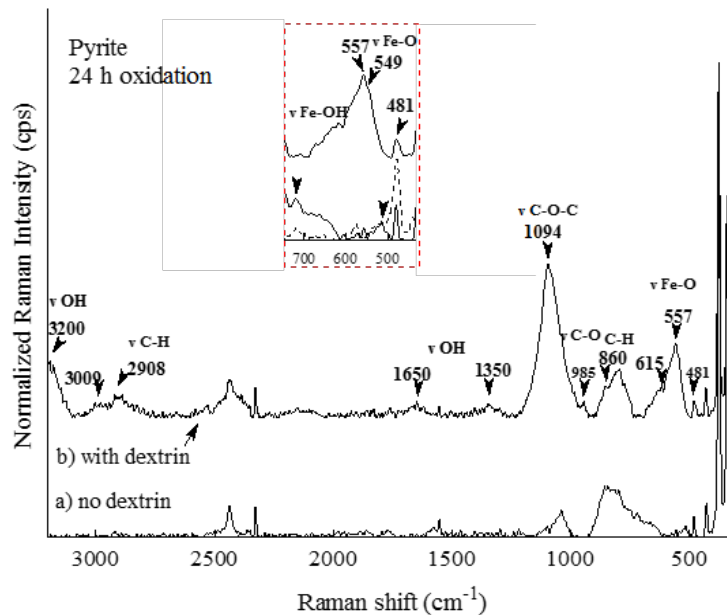

Fig. 6. Raman spectrum of pyrite oxidized for 24 h in the absence (a) and presence of dextrin (b)

on the pyrite oxidized for 30 min, because the surface density of ferrric hydroxide was higher. The adsorption isotherms presented two steps suggesting that dextrin adsorbed by two distinct mechanisms on the pyrite surface. These two-step isotherms differed from those reported so far for other sulfide minerals, which showed only one step (Wie and Fuerstenau, 1974; Liu and Laskowski, 1989; Nyamekye and Laskowski, 1993; Laskowski et al., 1993; Gärd et al., 1997; Bogusz et al., 1997; Rath et al., 2000; López Valdivieso et al., 2004).

Dextrin consists of a short chain linear glucopyranose fraction, amylose, and a long branched glucopyranose fraction, amylopectine. Fig. 7 shows the adsorption of such a mixture. Adsorption

preference occurs with respect to the molecular weight. High molecular polymers adsorb preferentially over lower molecular ones (Lyklema, 1995). In the first step of the adsorption isotherm, amylose and amylopectine can find place on highly reactive FeOH sites of the ferric hydroxide on the pyrite surface until saturation is reached. The second step of the adsorption isotherm may be due to preferential adsorption of the branched amylopectine on FeOH sites of lower energy.
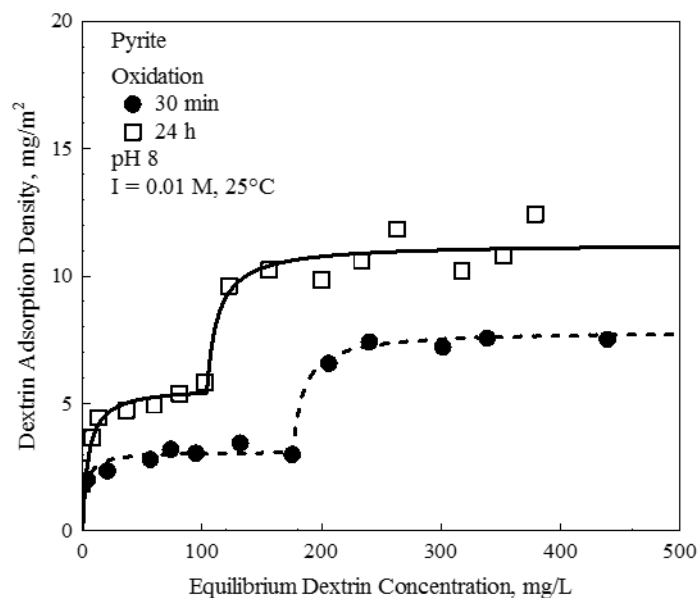

Fig. 7. Adsorption density of dextrin on oxidized pyrite for 30 min and 24 h
as a function of equilibrium dextrin concentration at pH 8

3.3. Xanthate adsorption on oxidized pyrite

Electrokinetics has been used to delineate the adsorption mechanism of xanthates on pyrite (Fuerstenau et al., 1968; Fuerstenau and Mishra, 1980; Fuerstenau et al., 1990; Fornasiero and Ralston, 1992; López Valdivieso et al., 2005). They all agree that xanthates adsorb on pyrite forming dixanthogen through the oxidation of xanthate ions. Oxygen (Ball and Rickard, 1976) and ferric hydroxide reduction (Lopez-Valdivieso et al., 2005) have been proposed to be the redox pair. In this work electrokinetic and Raman spectroscopic studies were undertaken to assess the xanthate adsorption on the oxidized pyrite.

Figure 8 shows the zeta potential of the oxidized pyrite as a function of pH in the absence and presence of two distinct concentrations of ethyl and propyl xanthates, namely 1×10^{-4} and 1×10^{-3} mol/dm^3. The zeta potential was not affected using the lowest xanthate concentration of 1×10^{-4} mol/dm^3, in agreement with Fuerstenau et al. (1968, 1990) and López Valdivieso et al., 2005. This is an indicative of dixanthogen formation on the pyrite surface since supposedly dixanthogen has no electric charge on its surface.

With the highest xanthate concentration of 1×10^{-3} mol/dm^3 the positive zeta potential of pyrite turned to negative within the pH range of 3.8 to 7.3. Fuerstenau et al. (1968, 1990) also observed this zeta potential behavior and López-Valdivieso et al. (2005) found that the zeta potential reversal was due to a decrease of ferric hydroxide on the pyrite surface by reduction to Fe^{2+} ions, coupled with the oxidation of xanthate ions to dixanthogen as follows:

$$2Fe(OH)_3(s, surf) + 2X^- + 6H^+ = X_2(surf) + 2Fe^{2+} + 6H_2O. \qquad (1)$$
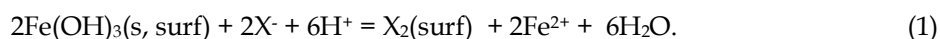
Fig. 9 shows the Raman spectra of the oxidized pyrite for 24 hs (a) and oxidized pyrite after treatment with ethyl (b) and propyl xanthate (c). In the Raman spectra of pyrite with the xanthates the bands at 2992-2845, 1040, 864, 662 cm^{-1} are due to the ν–CH, ν–COCS$_2$, ν–COC and ν–CS$_2$ groups (Parker and Hope, 2010), respectively, of the xanthates. This indicates the presence of xanthate on the pyrite. In addition, the bands at 491 and 496 cm^{-1} correspond to the S-S bond (Parker and Hope, 2010), which is due to dixanthogen. This verifies that xanthate adsorbed forming dixanthogen. The band at 720 cm^{-1} was of lower intensity than that of the oxidized pyrite in the absence of xanthate, indicating that the

amount of ferric hydroxide decreased on the surface of the pyrite treated with the xanthates in support to Eq. (1).
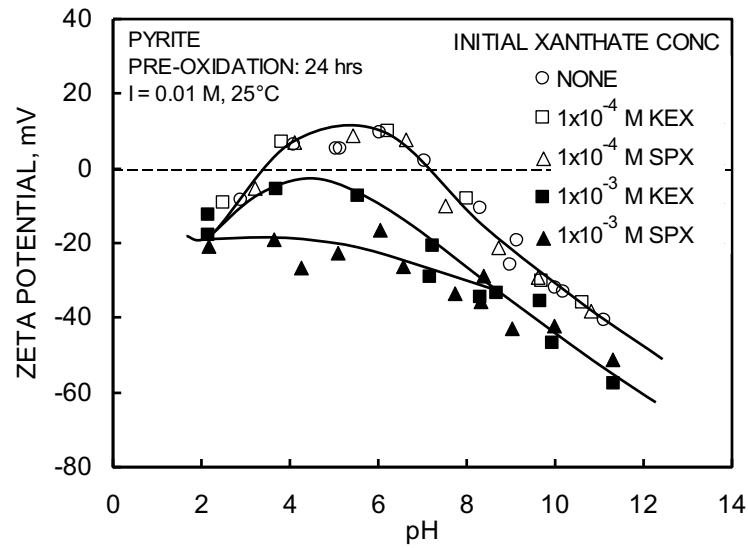

Fig. 8. Zeta potential of pyrite oxidized for 24 h as a function of pH in the absence and presence of 1x10-4 and 1x10-3 mol/dm3 ethyl (KEX) and propyl xanthate (SPX)
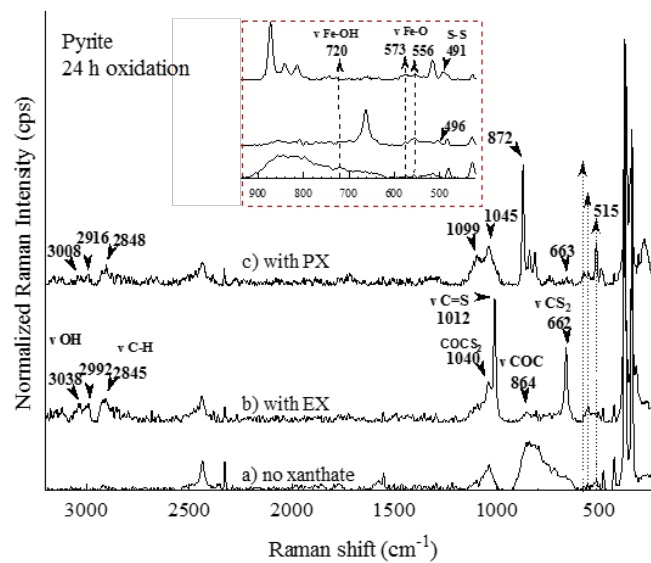

Fig. 9. Raman spectra of pyrite oxidized for 24 hs (a) then treated with ethyl xanthate (b) and propyl xanthate (c)

4. Dextrin and xanthate adsorption on oxidized pyrite

Dextrin adsorption increased with the surface density of ferric hydroxide. Upon xanthate adsorption the amount of surface ferric hydroxide decreased. Adsorption of ethyl and propyl xanthate as well as that of dextrin was assessed for the two oxidized pyrites. The pyrite was first contacted with dextrin followed by xanthate, then adsorption of both xanthate and dextrin was quantified.

Figure 10(a) depicts the dextrin adsorption isotherms on pyrite with 55 µmol/m² ferric hydroxide (30 min oxidation time) in the absence and presence of a constant initial concentration of 1x10-3 mol/dm3 of ethyl and propyl xanthates at pH 8. Fig. 10(b) shows the xanthate adsorption as a function of the equilibrium dextrin concentration. The dextrin adsorption isotherms and xanthate adsorption on pyrite with 81 µmol/m² ferric hydroxide (24 h oxidation time) are presented in Figs. 11(a) and 11(b), respectively.
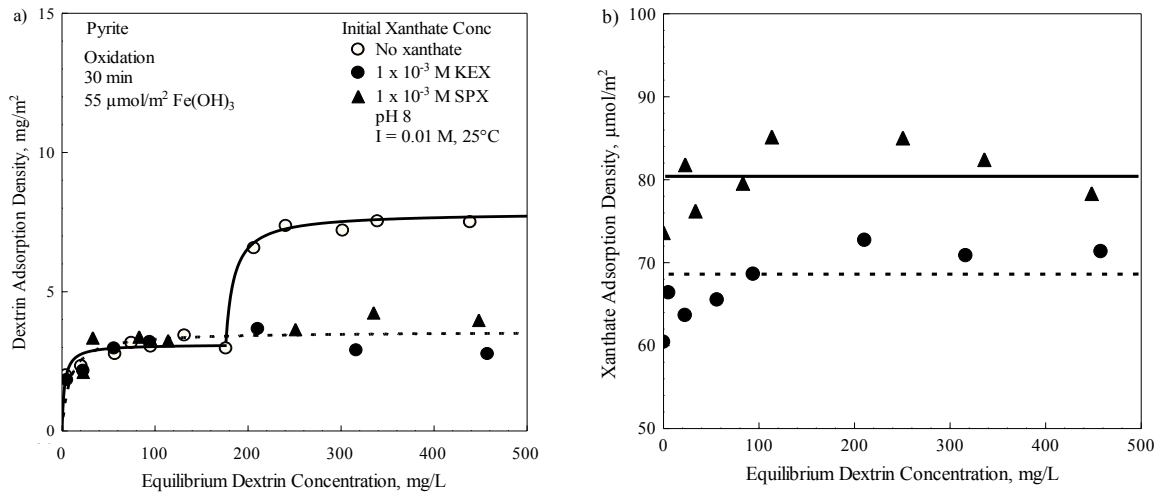
Fig. 10. (a) Adsorption density of dextrin on pyrite oxidized for 30 min as a function of equilibrium dextrin concentration in the absence and presence of 1x10⁻³ ethyl and propyl xanthate,
(b) adsorption density of ethyl and propyl xanthate on the oxidized pyrite as a function of equilibrium dextrin concentration (Lopez-Valdivieso et al., 2007)
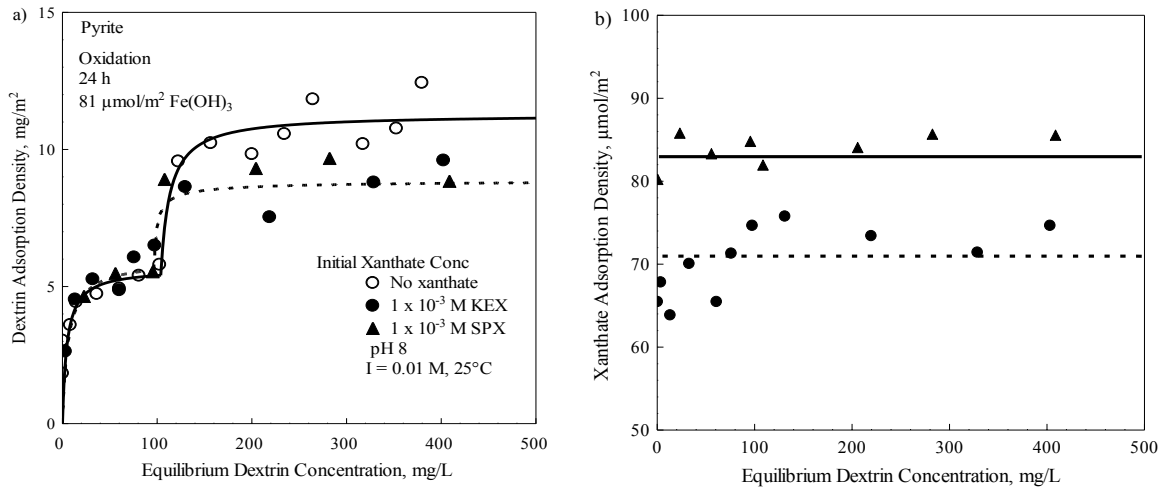

Fig. 11. (a) Adsorption density of dextrin on pyrite oxidized for 30 min as a function of equilibrium dextrin concentration in the absence and presence of 1x10⁻³ ethyl and propyl xanthate,
(b) adsorption density of ethyl and propyl xanthate on the oxidized pyrite as a function of equilibrium dextrin concentration (Lopez-Valdivieso et al., 2007)

Figs. 10(b) and 11 (b) show that ethyl and propyl xanthate adsorption was the same in the absence and presence of dextrin, indicating that dextrin did not inhibit the formation of dixanthogen on pyrite. Propyl xanthate adsorption was higher than that of ethyl xanthate as dixanthogen formation is more favorable for xanthates with a longer chain length (Woods, 1988). As noted in Figs. 10(a) and 11(a), the first step of the dextrin adsorption isotherm was not affected by the xanthates, but the second dextrin adsorption step decreased in magnitude by about 5 mg/m². Accordingly, dextrin desorption occurred along with the xanthate adsorption. Upon adsorption of xanthate, ferric hydroxide dissolved off from the surface of pyrite (Eq. 1) leading to the decrease of dextrin adsorption. Since there was still ferric hydroxide on the pyrite surface, dextrin co-adsorbed with the xanthates on the pyrite, in agreement with Miller et al. (1984) and López Valdivieso et al. (2004).

Fig. 12 shows the Raman spectra of oxidized pyrite dextrin treated (a) and after treatment with both dextrin and ethyl (b) and propyl (c) xanthates. In the spectrum of the pyrite treated with dextrin and ethyl xanthate, the band 1094 cm⁻¹ due to dextrin diminished significantly, indicating that dextrin

desorbed from the pyrite. On the other hand, the bands 492 and 496 cm-1, ought to dixanthogen, showed xanthate adsorption. Figure 13 shows a schematic of the co-adsorption of xanthate and dextrin on pyrite.
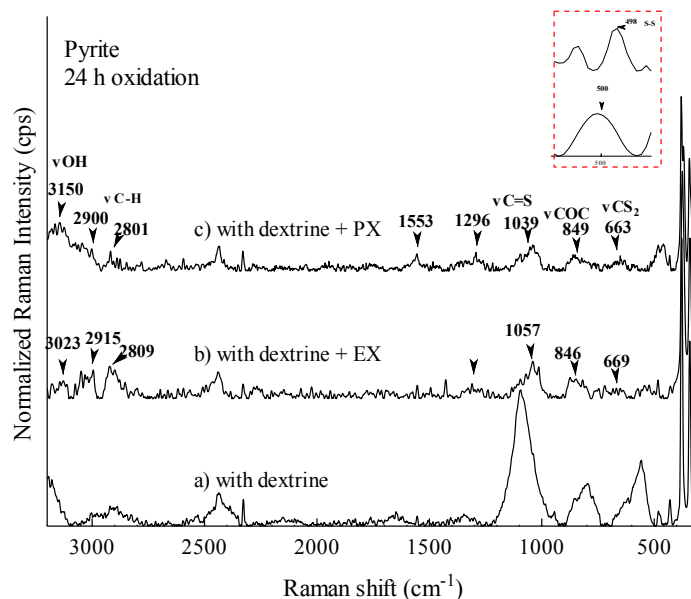

Fig. 12. Raman spectrum of oxidized pyrite for 24 h then treated with: (a) dextrin, (b) dextrin and ethyl xanthate and (c) dextrin and propyl xanthate
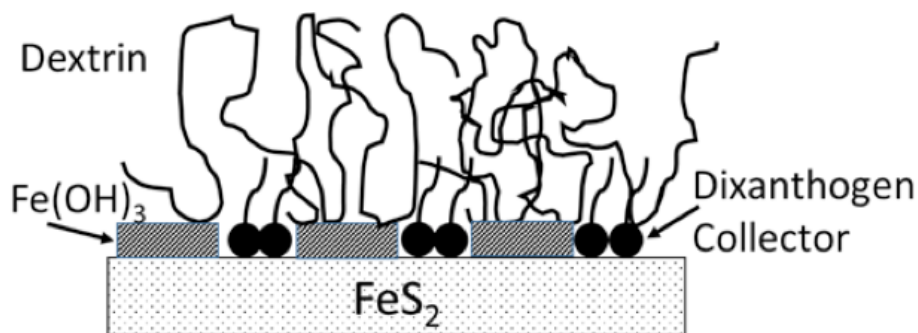

Fig. 13. Schematic of the co-adsorption of dextrin and xanthate on pyrite. Xanthate adsorbs as dixanthogen

3.4. Depression of pyrite floatability with dextrin

Dextrin on ferric hydroxide of the pyrite surface turns this surface hydrophilic, while dixanthogen resulting from xanthate adsorption renders the surface hydrophobic. Hence, to prevent pyrite flotation with dextrin in the presence of xanthates a condition needed is to have a high amount of ferric hydroxide on the pyrite surface to enhance dextrin adsorption.

Figure 14 shows the floatability of pyrite oxidized for 30 min and 24 hs as a function of dextrin concentration using $1x10^{-3}$ mol/dm^3 of ethyl and propyl xanthates at pH 8. As seen dextrin did not effectively impair the pyrite flotation when the pyrite was oxidized for only 30 min, because the surface density of ferric hydroxide was low, which brought about low dextrin adsorption on the pyrite. With 200 mg/dm^3 dextrin, the floatability of pyrite was 60 and 45% with propyl and ethyl xanthate, respectively. The higher pyrite floatability with propyl xanthate was because of a greater adsorption density of propyl xanthate in comparison to that of ethyl xanthate. So propyl xanthate converted the pyrite surface more hydrophobic and the hydrophilic effect of dextrin was less. On the other hand, effective depression was achieved above 50 mg/dm^3 dextrin for the pyrite oxidized for 24 hs as the surface density of ferric hydroxide was high causing high dextrin adsorption. Under these conditions, the pyrite surface became sufficiently hydrophilic by the dextrin and the hydrophobicity imparted by the adsorbed xanthate was overcome.
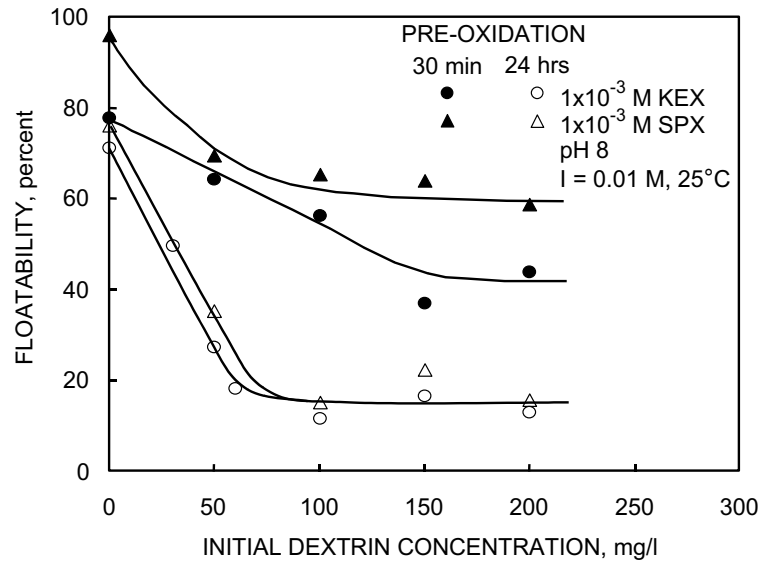
Fig. 14. Floatability of pyrite oxidized for 30 min and 24 h as a function of dextrin concentration in the presence of 1×10^{-3} mol/dm³ ethyl and propyl xanthate at pH 8

4. Conclusions

Dextrin and the collector xanthate co-adsorb on pyrite. Dextrin adsorption occurs through interaction with surface ferric hydroxide on the pyrite while the xanthate adsorbs as dixanthogen decreasing surface ferric hydroxide. Accordingly, xanthate decreases dextrin adsorption. Hence, the surface density of ferric hydroxide is key for pyrite depression by dextrin. The ferric hydroxide forms from the oxidation of pyrite and its surface density is highest about the isoelectric point of oxidized pyrite (pH 7.5). Then depression of pyrite by dextrin can be carried out effectively around this pH value and to assure high dextrin adsorption the surface density of ferric hydroxide on pyrite must be high. Under these conditions the surface hydrophilicity due to dextrin overcome the surface hydrophobicity created by the adsorbed collector.

Acknowledgements

References

BALL, B., RICKARD, R. S., 1976. *The Chemistry of Pyrite Flotation and Depression*. In: Fuerstenau M.C., Flotation A. M. Gaudin Memorial Volume 1, SME-AIME, 458–484.

BOGUSZ, E., BRIENNE, S. R., BUTLER, I., RAO, S. R., FINCH, J. A., 1997. *Metal ions and dextrin adsorption on pyrite.* Minerals Engineering 10, 441–445.

BUCLEY, A., WOODS, R., 1984. *An X-ray photoelectron spectroscopic investigation of the surface oxidation of sulfide minerals*. Proceedings of the International Symposium on Electrochemistry and Mineral Processing, The Electrochemical Society, 286–302.

BULUT, G., ARSLAN, F., ATAK, S., 2004. *Flotation behaviors of pyrites with different chemical compositions*. Minerals and Metallurgical Processing, 21, 86–92.

BULATOVIC, S. M., WYSLOUZIL, D. M., 1995. *Selection and evaluation of different depressants systems for flotation of complex sulphide ores*. Minerals Engineering 8, 63–76.

BULATOVIC, S. M., 2007. *Hand Book of Flotation Reagents. Chemistry, Theory and Practice: Flotation of Sulfide Ores* Vol 1. Elsevier, Amsterdam, 185-193.

CASTRO, S. 2012. *Challenges in flotation of Cu-Mo sulfide in sea water. In: Water in Mineral Processing*. Proceedings of the 1st International Symposium, J. Drelich (Ed.) SME, Englewood, Colorado, USA, 29-40

CHANDER, S., 1988. *Inorganic depressants for sulfide minerals. In: Reagents in Mineral Technology*, Surfactant Science Series Vol 27. Somasundaran P., Moudgil B. M. (Eds.), Marcel Dekker, New York, 429–469.

CLARKE, P., FORNASIERO, D., RALSTON, J., SMART, R. St. C., 1995. *A study of the removal of oxidation products from sulfide mineral surfaces*. Minerals Engineering, 8, 1347–1357.

DAS, D., MUKHERJEE, S., PAL, A., DAS, R., SAHU, S.G. PAL, S., 2016, *Synthesis and characterization of biodegradable copolymer derived from dextrin and poly(vinyl acetate) via atom transfer radical polymerization*, RSC Advances, 6, 9352-9359

DAS, S. HENDRY, M., 2011, *Application of Raman spectroscopy to identify iron minerals commonly found in mine wastes*. Chemical Geology, 290, 101-108.

DUBOIS, M., GILLES, K. A., HAMILTON, J. K., REBERS, P. A., SMITH, F., 1956. *Colorimetric method for determination of sugars and related substances*. Anal. Chem., 28, 350–356.

FORNASIERO, D., RALSTON, J., 1992. *Iron hydroxide complexes and their influence on the interaction between ethyl xanthate and pyrite*. Journal of Colloid and Interface Science, 151, 225–235.

FUERSTENAU, M. C., KUHN, M. C., ELGILLANI, D. A., 1968. *The role of dixanthogen in xanthate flotation of pyrite*. AIME Transactions, 241, 148–156.

FUERSTENAU, M. C., NATALIE, C. A., ROWE, R. M., 1990. *Xanthate adsorption on selected sulfides in the virtual absence and presence of oxygen*. Int. J. Miner. Process., 29, 89–119.

FUERSTENAU, D. W., METZGER, P. H., SEELE, G. D., 1957. *Modified Hallimond tube for flotation testing*. Engineering and Mining Journal, 158, 93–95.

FUERSTENAU, D. W., MISHIRA, R. K., 1980. *On the mechanism of pyrite flotation with xanthate collectors. In: Complex Sulfide Ores*. Jones J. J.(Ed.) The Institution of Mining and Metallurgy, London, 271–278.

GARD, R., HOLMGREN, A., FORSLING, W., 1997. *Spectroscopic studies of dextrin adsorption onto colloidal ZnS*. Journal of Colloid and Interface Science 194, 319–325.

HOCHELLA, M. F., 2003. *Nanoscience and technology: The next revolution in the earth sciences, earth and planetary science letters*, Vol. 203, 593–605.

KYDROS, K. A., GALLIOS, G. P., MATIS, K. A., 1994. *Modification of pyrite and sphalerite flotation by dextrin*. In: Separation Science and Technology, Marcel Dekker, Inc., Vol. 29, 2263–2275.

LASKOWSKI, J. S., SUBRAMANIAN, S., NYAMEKYE, G. A., 1993. *Polysaccharides – emerging non-toxic modifiers for differential flotation of sulphides*. XVIII International Mineral Processing Congress, Sydney, Australia, 593–600.

LEJA, J., 1982. *Flotation surfactants*. In: *Surface chemistry of froth flotation*, Plenum Press, New York, 228–258.

LIN, K. P., BURDICK, Ch. L., 1988. *Polymeric Depressant*. In: *Reagents in Mineral Technology*, Surfactant Science Series Vol 27. Somasundaran, P., Moudgil, B. M. (Eds.). Marcel Dekeer Inc., New York, 471-484.

LIU, Q., LASKOWSKI, J. S., 1989. *The role of metal hydroxides at mineral surfaces in dextrin adsorption*. I. Studies on modified quartz samples, Int. J. Miner. Process. 26, 297–316.

LIU, Q., LASKOWSKI, J. S., 2002. *Adsorption of polysaccharides on mineral surfaces from aqueous solutions*. In: *Encyclopedia of Surface and Colloid Science*, A. T. Hubbard (Ed.), Marcel Dekker, New York, 573–590.

LOPEZ-VALDIVIESO, A., SANCHEZ-LOPEZ, A. A., SONG, S., GARCIA MARTINEZ, H. A., LICON-ALMADA, S., 2007. *Dextrin as a regulator for the selective flotation of chalcopyrite, galena and pyrite*. Canadian Metallurgical Quaterly, 46(3) 301-307.

LOPEZ-VALDIVIESO, A., SANCHEZ-LOPEZ, A. A., SONG, S., ROBLEDO-CABRERA, A., CELEDON-CERVANTES, T., 2003. Flotation chemistry of pyrite with xanthates as collector and dextrin as a depressant. Copper 2003-Cobre 2003, Vol. III-Mineral Processing, C. O. Gomez and C. A. Barahona (Eds.), Santiago, Chile, 283–297.

LOPEZ-VALDIVIESO, A., CELEDON-CERVANTES, T., SONG, S., ROBLEDO-CABRERA, A., LASKOWSKI, J. S., 2004. *Dextrin as a non-toxic depressant for pyrite in flotation with xanthates as collector*. Minerals Engineering, 17, 1001–1006.

LOPEZ-VALDIVIESO, A., SANCHEZ LOPEZ, A. A., SONG, S., 2005. *On the cathodic reaction coupled with the oxidation of xanthates at the pyrite/aqueous solution interface*. Int. J. Miner. Process., 77, 154–164.

LYKLEMA, J. 1995. Fundamentals of interface and Colloid Science, Vol II: Solid-Liquid Interfaces. Academic Press, San Diego, California, Chapter 5.

MILLER, J. D., LIN, C. L., CHANG, S. S., 1984. *Coadsorption phenomena in the separation of pyrite from coal by reverse flotation.* Coal Preparation, 1, 21–38.

MILLER, J. D., DU PLESSIS, R., KOTYLAR, D. G., ZHU, X., SIMMONS, G. L., 2002. *The low-potential hydrophobic state of pyrite in amyl xanthate flotation with nitrogen.* Int. J. Miner. Process., 67, 1–15.

NYAMEKYE, G. A., LASKOWSKI, J. S., 1993. *Adsorption and electrokinetic studies on the dextrin-sulfide mineral interactions.* Journal of Colloid and Interface Science, 157, 160–167.

PARKER, G. K. HOPE G. A., 2010. *A Raman Spectroscopic Investigation of Pyrite Oxidation and Flotation Reagent Interaction*, Electrochemical Society Trans. 28, 39-50.

RATH, R. K., SUBRAMANIAN, S., 1999. *Adsorption, electrokinetic and differential flotation studies on sphalerite and galena using dextrin.* Int. J. Miner. Process., 57, 265–283.

RATH, R. K., SUBRAMANIAN, S., PRADEEP, T., 2000. *Surface chemical studies on pyrite in the presence of polysaccharide-based flotation depressants.* Journal of Colloid and Interface Science, 229, 82–91.

RUMBALL, J. A., RICHMOND, G. D., 1996. *Measurement of oxidation in a base metal flotation circuit by selective leaching with EDTA.* Int. J. Miner. Process., 48, 1–20.

SITTER, A. J., SHIFFLETT, J. R. TRENER, J., 1988, *Resonance Raman Spectroscopic Evidence for Heme Iron-Hydroxide Ligation in Peroxidase Alkaline Forms*, The Journal of Biological Chemistry, 263 (26), 13032-13038.

STONE, K. L., BEHAN, R. K. GREEN, M. T., 2006, *Resonance Raman spectroscopy of chloroperoxidase compound II provides direct evidence for the existence of an iron(IV)–hydroxide*, Proceedings of the National Academy of Sciences, 103 (33), 12307-12310.

TODD, E. C., SHERMAN, D. M., PURTON, J. A., 2003. *Surface oxidation of pyrite under ambient atmospheric and aqueous (pH=2 to 10) conditions: Electronic structure and mineralogy from X-ray absorption spectroscopy.* Geochimica et Cosmochimica Acta, 67, 881–893.

WANG, X., FORSSBERG, E., 1990. *EDTA-induced flotation of sulfide minerals.* Journal of Colloid and Interface Science, 140, 217–226.

WIE, J. M., FUERSTENAU D. W., 1974. *The effect of dextrin on surface properties and the flotation of molybdenite.* Int. J. Miner. Process., 1, 17–32.

WIESSENBORN, P. K., 1993. *Selective flocculation of ultrafine iron ore*, Ph. D. Thesis, Curtin University of Technology.

WOODS, R. 1988. *Flotation of sulfide minerals.* In: Reagents in Mineral Technology, Surfactant Science Series Vol 27. Somasundaran, P., Moudgil, B. M. (Eds.). Marcel Dekeer Inc., New York. 39-78.